Journal of Hazardous Materials 164 (2009) 432–441

Contents lists available at ScienceDirect

Journal of Hazardous Materials

journal homepage: www.elsevier.com/locate/jhazmat

Nitric oxide removal from flue gas with a biotrickling filter using *Pseudomonas putida*

Ran Jiang, Shaobin Huang*, Alex T. Chow, Jun Yang

College of Environmental Science and Engineering, South China University of Technology, University City, Guangzhou 510006, PR China

ARTICLE INFO

Article history:
Received 22 May 2008
Received in revised form 6 August 2008
Accepted 6 August 2008
Available online 26 August 2008

Keywords:
Nitric oxide
Pseudomonas putida
Aerobic denitrification
Biotrickling filter

ABSTRACT

The development of an effective biotrickling filter (BF) system to inoculate a newly isolated strain of *Pseudomonas putida* SB1 for the effective treatment of nitric oxide (NO) is described. The experiments were carried out in a bench-scale BF under high concentrations of O_2 and NO in simulated flue gas. A method including alternating aeration in screening and rescreening based on the pH changes for cultivating natural aerobic denitrifying bacteria was employed. The SB1 showed a denitrifying capability of 95% nitrate removal rate over a 24 h period in an aerobic environment, with no nitrite accumulation. The BF system was able to consistently remove 82.9–94.2% NO when the inlet NO was 400 ppm in an enriched oxygen stream of 2–20%. The oxygen had no negative effect on the aerobic denitrifier SB1, but rather enhanced the total efficiency in part by chemical oxidation and in part by the strain activities. A kinetic relation between the oxygen concentration and biological NO removal was developed to confirm that the microbial metabolism played the main role. 79.3% of the total NO removal can be attributed to bio-denitrifying at 20% oxygen, and most chemical oxidation occurred concurrently. Overall, the study demonstrates that NO removal by the aerobic denitrifying process in BF is feasible in flue gas.

1. Introduction

Nitrogen oxides (NOx) generally refer to six compounds of nitrogen and oxygen, namely N_2O, NO, NO_2, N_2O_5, N_2O_3, and NO_5. However, it often refers specifically to the two common compounds: nitric oxide (NO) and nitrogen dioxide (NO_2). NOx, together with sulfur dioxide (SO_2) are hazardous air pollutants that lead to the formation of acid rain, airborne particulates, and increased ground level ozone [1]. Emissions of NOx in China have undergone an almost exponential increase over the past decade. In the year 2004, NOx emissions from its electricity industry alone exceeded 6.65 million tons. Continuing the current trend, NOx emission would reach 7.13 million tons in the year 2010 [2].

Traditional controls, such as selective catalytic reduction and selective non-catalytic reduction, are currently used to control power plant NOx emissions. However, both processes require high temperatures or the use of catalysts, creating high installation and maintenance costs. This cost is prohibitive for large-scale treatment of air containing low to moderate concentrations of NOx [3].

A biotrickling filter (BF) used in biological NOx treatment is a promising alternative. However, the development of this technology offers unique challenges. Flue gas in a coal power plant stack consists of CO_2, SOx, NOx, O_2, and suspended particles. Of these the pollutants are primarily SOx and NOx, with about 90% being NO of low solubility [4–6]. Biotrickling filters (BFs) containing inert packing material (such as ceramics, compost) could provide sufficient surface area for gas/liquid mass transfer and biofilm growth. These BFs have been applied to the treatment of gas streams containing volatile ethanol [7], sulfur compounds [8] and mercury [9] from flue gases. Biofiltration incubated bacteria indigenous to compost or soil are credited with removing up to 85% of the NO from an oxygen-free simulated flue gas using denitrifying microbial populations [3,10–12].

Denitrification is a dissimilatory reductive process that occurs in the following simplified order: $NO_3^- \rightarrow NO_2^- \rightarrow NO \rightarrow N_2O \rightarrow N_2$. Thus denitrifying bacteria use toxic nitrogen oxides to produce environmentally benign nitrogen gas. Denitrifying bacteria such as *Paracoccus denitrificans* and *Pseudomonas denitrificans* have this function in an anaerobic environment [3]. However, concentrations of up to 10% oxygen in flue gas inhibits the removal of NOx compounds by typical denitrifying bacteria [3]. Removal efficiency (RE) at a level greater than 50% occurs in an oxygen-free environment, but was reduced to less than 20% when 2% oxygen was introduced into the gas–stream [13]. Aerobic denitrification has been positive using pure strains like *Thiosphaera pantotropha* and *Microvirgula aerodenitrificans* [14,15]. Hence the BF inoculated aerobic denitrifier

* Corresponding author. Tel.: +86 20 39380587; fax: +86 20 39380577.
E-mail address: chshuang@scut.edu.cn (S. Huang).

0304-3894/$ – see front matter © 2008 Elsevier B.V. All rights reserved.
doi:10.1016/j.jhazmat.2008.08.058

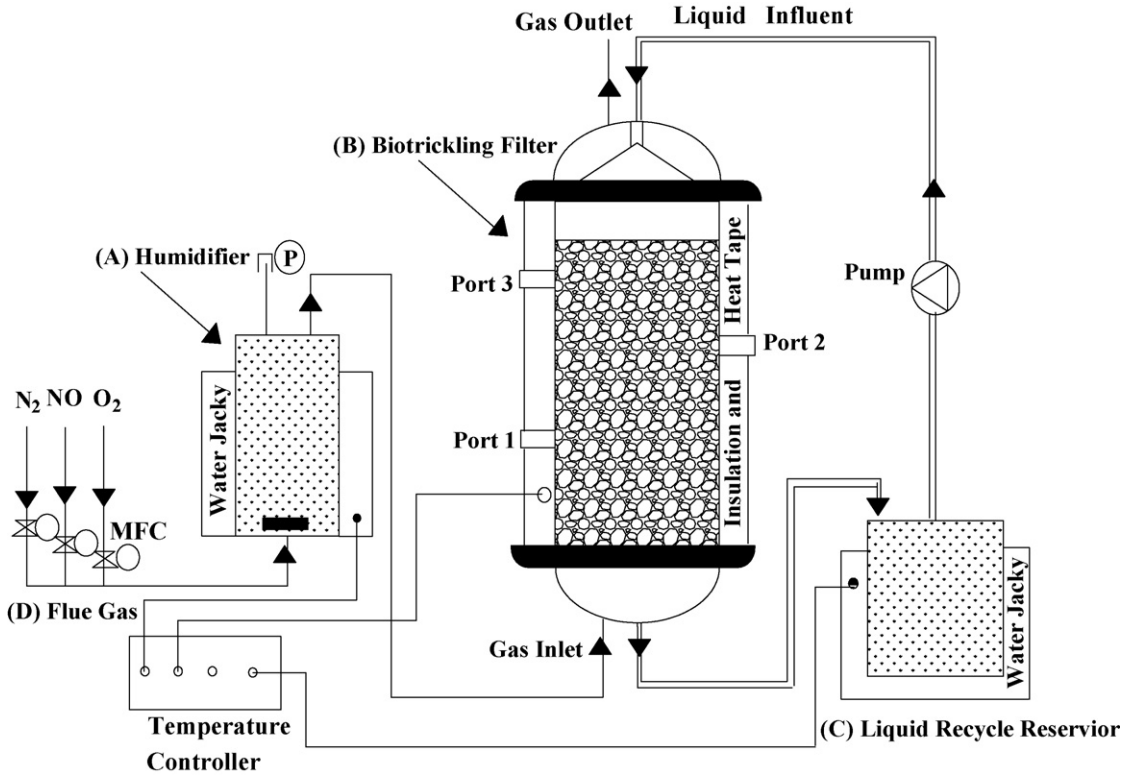

Fig. 1. Schematic of the biotrickling filter system.

is an alternative for NOx removal in flue gas. NO might be responsible for a cumulative induction of the denitrification enzyme nitrite reductase and NO reductase as has been shown for *Pseudomonas fluorescens*, leading to high aerobic denitrification rates [16,17]. Zart and Bock [18] found that the addition of NO_2 or NO to *Nitrosomonas eutropha* leads to a significant enhancement of the nitrification, the denitrification, and the cell growth.

Degradation of phenol by *Pseudomonas putida* is well documented [19–21]. However, as far as we know, the *P. putida* denitrifying potential for NO removal from flue gas has not yet been explored. Therefore this study inoculates *P. putida* to the BF to evaluate its denitrifying capability and NO removal efficiencies.

Development of an effective bench-scale BF system inoculated with a newly isolated strain of *P. putida* SB1 is described for the effective treatment of NO from simulated gas–streams under a high concentration of oxygen. The research observed biofilm formation to generate a viable startup of the system, then checked the efficiencies of the BF in 2–20% O_2 and 50–400 ppm NO concentrations. The high end of the O_2 range exceeds that found in flue gas today.

2. Materials and methods

2.1. Biotrickling filter system design

Fig. 1 schematically represents the BF system used in this study. It basically consists of (A) a humidifier, (B) a BF and (C) a liquid recycle reservoir. NO, N_2 and O_2, the main components in flue gas after wet flue gas desulfurization, were supplied from compressed gas cylinders, then mixed in the humidifier (A) before entering the BF (B). The flux of NO, N_2 and O_2 was controlled by a mass flow controller (MFC, D07-7B, Sanxing, China).

The total height of the BF was 50 cm with an inner diameter of 8 cm and a bed depth of 30 cm. Three sample ports were located 3, 15, and 28 cm from the bottom, respectively (Fig. 1). The clear, acrylic inner chamber of the BF was filled with packing material and the outside wrapped with heat tape, then wrapped with a 1 cm layer of fiberglass for insulation. The heat tape was controlled by a digital temperature controller using a thermostat inserted into the biofilter packing as an input signal. While the BF had been operating for a long time, the ambient temperatures fluctuated in the range of 7–28 °C. To avoid more variability in this research, the temperature was controlled at 30 °C. For incubation temperature in this research it was also set to the same temperature. The BF was operated at constant ambient temperature (30 ± 0.5 °C). The constant volume (5 L) liquid recycle reservoir (C) was controlled at 30 ± 1 °C by means of a water jacket. To maintain the humidity saturation in the simulated flue gas (D), an ultrasonic nebulizer unit, capable of delivering a fine spray to the BF, was located at the bottom of the humidifier. The humidifier has half the volume of the BF. Gas entered the BF from the bottom, while a peristaltic pump supplied the filter with nutrient liquid from the top.

2.2. Inoculum preparation

2.2.1. Screening of aerobic denitrifiers

Aerobic denitrifying organisms were enriched from the second sludge sample obtained from an anoxic-anaerobic-oxic waste water treatment process at the Liede Waste Water Treatment Plant (Guangzhou, China). The sludge samples were inoculated in a lab-scale sequencing batch reactor (SBR) in which the total volume was about 3 L, with 2 L of enrichment media (EM). EM was fed to the SBR in 24 h cycles. Each cycle included periods of aeration, sludge settling, discharging and loading. The initial mixed liquor suspended solids (MLSS) in the SBR was about 10 g/L and dissolved oxygen (DO) was 4.8–5.2 mg/L. The initial aeration time lasted 3.5 h per day, with aeration time increasing as the total nitrogen (TN) removal rate increased. The charcoal grey granular sludge turned light grey and flocculent by the end of the first screening. Research has shown that

there is no specific natural ecological niche for aerobic denitrifiers. But when selective variable manipulation such as alternating aeration is applied, the flexible nitrate–oxygen metabolism is amplified, where a nitrate or NO is used as the electron acceptor for the respiration of organic matter [14,17].

After TN RE reached 90%, the settled sludge was collected for a second screening. Ten milligrams of the sludge was put into 100 mL of the EM in 200 mL flasks with nine layers of gauze. Several sterilized glass beads were added to destroy the sludge floc aggregate in order to prevent an anaerobic microenvironment. The flasks were inoculated at 30 °C on a rotary shaker at 120 rpm. This procedure was repeated three times. Nitrate consumption, pH increase and bubble formation indicated denitrification. The resultant bacterial suspension was streaked on bromothymol blue (BTB) medium agar plates and incubated at 30 °C for 3 days. The isolation of aerobic denitrifiers was based on the changes in the pH of the BTB medium. Positive strains consuming the nitrates caused an increase in pH from 7.0 to above 7.6. Blue colonies and/or halos were obtained and screened further based on the pH indicator BTB [22]. This rescreening was repeated three times. The incubated BTB medium plates changed from white to blue after 2 days during the final isolation. Six strains were obtained from the screenings and the most successful denitrifying strain was named SB1.

In order to enhance NO reduction in an aerobic environment, SB1 was incubated in 200 mL flasks containing the mineral medium, sealed with a butyl rubber stopper, then rotary shaken at 120 rpm at 30 °C. O_2 concentrations of 2, 4, 6, and 8% by volume and 100 ppm NO were used to replace air in the flasks. Air was also pumped in to form positive pressure. The aerobic denitrification by the microorganism was measured by determining the time-dependent production of nitrate, nitrite, the amount of residual O_2 and NO in the headspace gas.

2.2.2. Bacterial identification

The 16S rRNA sequence of SB1 was determined by a sequencing amplified polymerase chain reaction (PCR) 16S rRNA. The total bacterial DNA was extracted from each isolate and purified as described by Ozeki et al. [23]. The genes encoding 16S rRNA were amplified by using the total DNA (0.1 μg) as the template. The primers used for PCR amplification were F27 (*Escherichia coli* numbering 8-27: 5′-AGAGTTTGATCATGGCTCAG-3′) and R1522 (*E. coli* numbering 1522-1541: 5′-AAGGAGGTGATCCAGCCGCA-3′) [24]. Genes were amplified by 30 cycles of denaturation at 94 °C for 1 min, annealing at 56 °C for 1 min, and extension at 72 °C for 2 min, followed by final extension at 72 °C for 7 min. The PCR products were sequenced by Invitrogen Company (Shanghai, China). The 16S rRNA sequences were examined in blastn (NCBI, USA) for similarities.

2.2.3. Media

The media used in inoculation were EM and BTB mediums, and trace element solutions. The ingredients of the EM were as follows (g/L): KNO_3, 5.0; $Na_2HPO_4{\cdot}7H_2O$, 7.9; KH_2PO_4, 1.5; NH_4Cl, 0.3; $MgSO_4{\cdot}7H_2O$, 0.1; Na-succinate, 10; trace element solution, 2 mL; pH 7–7.5. The ingredients of the BTB medium were as follows (g/l): KNO_3, 10.0; $Na_2HPO_4{\cdot}7H_2O$, 7.9; KH_2PO_4, 1.5; $MgSO_4{\cdot}7H_2O$, 0.1; Na-succinate, 15; BTB (1% in ethanol), 1 mL; agar, 8 g; trace element solution, 2 mL; pH 7.0. The trickling liquid consisted of a nutrient medium with the following composition used for startup and NO removal (g/L): glucose, 2.0; KNO_3, 1.0 (in startup stage) or 0–0.5 (in NO removal operation); $Na_2HPO_4{\cdot}7H_2O$, 3.0; KH_2PO_4, 1.5; $MgSO_4{\cdot}7H_2O$, 0.1; NaCl, 4.7; trace element solution, 2 mL; pH 7–7.5. The trace element solutions for the bacteria growth included the following components (g/L): EDTA, 50.0; $ZnSO_4$, 2.2; $CaCl_2$, 5.5; $MnCl_2{\cdot}4H_2O$, 5.06; $FeSO_4{\cdot}7H_2O$, 5.0; $(NH_4)_6Mo_7O_2{\cdot}4H_2O$, 1.1; $CuSO_4{\cdot}5H_2O$, 1.57; $CoCl_2{\cdot}6H_2O$, 1.61; pH 7.0. All the chemicals were analytical grade reagents, commercially available and used without further purification. NO (99.9%) was obtained from Foshu Kede Gas Co. N_2 (99.99%) and O_2 (99.99%) were obtained from the Guangzhou Gas Co.

2.3. Packing material

Porous ceramic beads and polyhedral spheres made of polypropylene were used as packing material. The porous ceramic beads had an average aggregate diameter of 2–3 mm (void fraction is about 0.35), which were microporous giving surface and retention properties favorable to microbe growth. However, their dense packing resulted in a significant pressure drop of 500–520 Pa/m when the inlet airflow was 60 L/h. The polyhedral spheres (diameter of 5 cm, void fraction is 0.90), while not as favorable to microbe growth, only caused an 85 Pa/m pressure drop under the same condition. Therefore to reduce the pressure drop and still enhance colonization, an equal mixture by volume of the two packing mate-

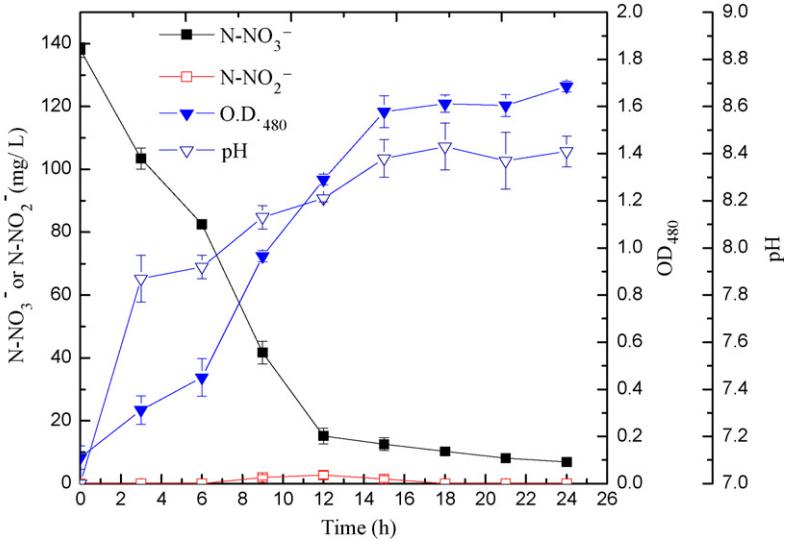

Fig. 2. Temporal variation of nitrite and nitrate concentration, the value of pH and $O.D._{480}$ for aerobic denitrification of strain SB1 (T = 30 °C, DO = 6.5–5.3 mg/L).

rials was used, resulting in less than a 350 Pa/m pressure drop, and reaching an average porosity of the filter bed of about 0.65.

2.4. Analytical methods

The NO, NO_2, and O_2 concentrations at both the inlet and outlet were analyzed by a flue gas analyzer (TESTO 350pro, Germany) at 8 h intervals. This instrument is capable of determining the concentration of NO and NO_2, either separately or together as NOx. The NO was measured prior to entering the humidifier to obtain the unoxidized value for NO, then again at the inlet and outlet of the BF. In this study, nitrate, nitrite and chemical oxygen demand (COD) were determined using the standard methods [25]. DO and pH were measured with a multi-function water quality monitor (Mnlti 340i, Germany WTW). Optical density ($O.D._{480}$) was determined by spectrophotometry (TU1810, Pgeneral, China) at a wavelength of 480 nm. Microbial counts were done in duplicate on EM/nitrate agar medium plates. A dilution series of biofilm and recycled liquid samples were prepared in 8.5 g/L NaCl for plates incubated at 30 °C. A phase-contrast microscope (CF-2010C, Shanghai, China) was used to estimate the biofilm thickness. An abiotic experiment was also conducted to estimate biological NO removal. In this study, a confidence limit of 95% was used, and all experimental results represent the mean of at least three runs.

SEM observation: the morphology of the bacteria and biofilm were examined with an environmental scanning electron microscope (XL30, Philips, ESEM). The samples were pretreated by fixing with 2.5% pentanediol in a 0.1 M phosphate buffer, then soaked in 1% osmic acid. Subsequently, the samples were washed and dehydrated in a graded series of ethanol solutions (50, 70, 80, 90 and 100%). The samples were dried by the critical point method and coated with gold.

3. Results and discussions

3.1. Characterization of P. putida SB1

The time for nitrate, nitrite reduction and the growth of strain SB1 are shown in Fig. 2. Strain SB1 grew in EM (1 g/L KNO_3) under aerobic conditions (shaking frequency 160 rpm. DO range from 6.5 to 5.3 mg/L). Cell growth exhibited no distinct lag phase at the beginning of cultivation. When cell growth reached the exponential phase, the cell concentration increased quickly from 0.11 $O.D._{480}$ to 1.29 $O.D._{480}$, and the nitrate concentration decreased sharply from 138.52 to 15.13 mg/L with no accumulation of nitrite. Nitrite peaked at 2.7 mg/L after 12 h of cultivation. While the pH increased from 7 to 8.2 at the exponential phase, there was no significant change during the stationary phase. Rich bubbles in the flasks after 18 h denoted the denitrifying gas product. After 24 h the nitrate in EM had decreased to 6.89 mg/L from the initial 138.52 mg/L (95% RE) and the experiment was terminated. A control experiment which omitted shaking showed only 87.3% removal in the 24 h. Thus strain SB1 grew better under an aerobic condition than under a stationary condition.

The partial 16S rRNA sequences of the isolated strain SB1 are identical to *P. putida* (99.8% homology). After taxonomical characterization, the results of morphological, physiological and biochemical tests are summarized in Table 1. From Fig. 3, picturing *P. putida* SB1 on EM/nitrate agar medium plates incubated under aerobic conditions, its cells are seen to be short rod shaped. While most fall between 0.5 and 1.5 μm, some are 1.5–2 μm in the cell-cleavage stage.

Table 1
Taxonomical characteristics of the aerobic denitrifying strain SB1

Test	Result
Morphological test	
Colony morphology	Round
Margin	Regular
Elevation	Raised
Surface	Smooth
Density	Opaque
Pigment	Light yellow
Gram's reaction	–
Shape	Rod
Size	Short
Arrangement	Single
Physiological test	
Growth temperature (°C)	4–40
Growth pH	6.0–11.0
Growth under anaerobic condition	+
Biochemical test	
Oxidation/fermentation (O/F)	O
Catalase test	+
Phenylalanine ammonialyase	–
H_2S production	–
Voges Proskauer test	–
Gelatin liquefaction	–
Nitrate reduction	+
Nitrite reduction	+
Lysine decarboxylase	–
O-Nitrophenyl-β-D-galactopyranoside	–
Methyl red test	–
Arginine dihydrolase	+
Lecithase test	–
Citrate utilization	+
Urea hydrolysis	+
Indole test	–
Acid production from carbonhydrates	
Arabinose	–
Cellobiose	+
Dextrose	+
Dulcitol	–
Fructose	+
Lactose	+
Sucrose	+

(+), positive reaction; (−), negative reaction.

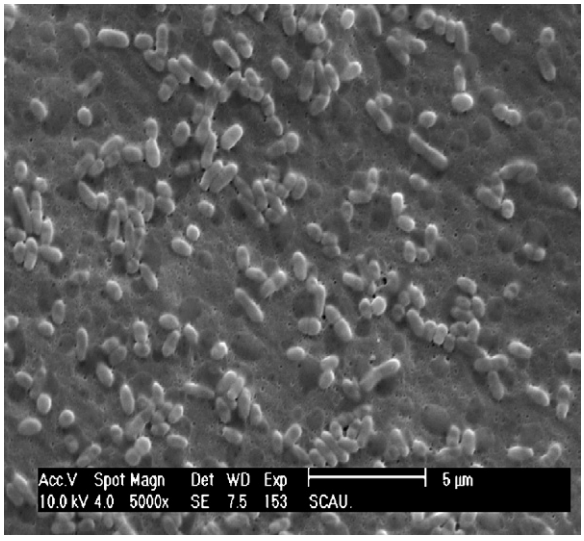

Fig. 3. Micrographs of strain SB1 grown on EM/nitrate agar medium plates after 3 days of incubation by SEM observation (T = 30 °C).

Table 2
Startup operating strategies and biofilm formation

Day	Procedure	Observation
1–50	The trickling rate is 200 mL min^{-1}, 30% of the trickling liquid is replaced every other day	Macroscopic yellow biofilm. The denitrifying rate decreased stepwise
1–30	The trickling rate is 200 mL min^{-1}, 30% of the trickling liquid is replaced every other day. The inlet and outlet gases were passed through sterile 0.45 μm bacterial air vents	No visible macroscopic biofilm. The denitrifying rate remained high
1–20	The trickling and soaking packing were intermittent in the first 10 days. The trickling rate was 200 mL min^{-1} in the remaining 10 days. However, 50% of the trickling liquid was replaced every other day	Macroscopic yellow biofilm. The denitrifying rate remained high

3.2. Startup of the biotrickling filter

After inoculation of the BF with the strain *P. putida* SB1 solution ($O.D._{480}$ = 1.6), various attempts were made to shorten the startup phase. First it was found that the NO injection was unnecessary until after the denitrifying rate reached 80% and macroscopic yellow biofilm was observed. After that KNO_3 was used to replace NO, then it and glucose were used as the nitrogen and carbon sources, respectively, to maintain biomass growth. For the startup, three operational strategies were tested (Table 2). BFs are, in general, more difficult to start than biofilters because the cultures need to attach to inert packing, and form a biofilm to overcome being washed away, as they are subject to shear stress from downward water flow.

As is shown in Fig. 4a, the denitrifying rate decreased stepwise from the maximal 80.5% RE at 16 days to poor efficiency (18.5%) at 28 days after which the system was shut down. The biofilm morphology was changed by an unknown microorganism growing on the packing surface. The diameter of the microorganism ranged from 12 to 15 μm. Note that *P. putida* has an average diameter of 0.5–1.5 μm as observed by SEM. COD was used to reflect the glucose concentration. That the COD removal reached 82% and corresponded to only about 20% nitrate removal indicated that the alien microorganisms had utilized most of the nutrient ingredients and SB1 lost its dominance. Thus the initial startup failed when the alien bacteria invaded the dominant community via the gas outlet.

In the second startup, in order to avoid alien interference, the inlet and outlet gases were passed through sterile 0.45 μm bacterial air vents. Then the SB1 liquid was incubated in the recycling nutrient liquid for the second time. During the entire second startup stage, the system maintained a denitrification rate above 80%. However, after one month there was little biofilm formation, and the second stage failed when the amount of SB1 in the liquid was larger than that growing on the packing surface by two or three orders of magnitude. According to biofilm formation theory, the initial step in biofilm formation is a non-specific, reversible attachment of bacteria to the packing surfaces. Once this attachment becomes permanent, the bacteria start to synthesize insoluble exopolysaccharides (EPS) that encase the adherent bacteria into colonies. With the accumulation of EPS and the reproduction of bacteria, the colonies develop into mature biofilm [26]. As shown in Fig. 4b, when the SB1 concentration in the liquid was at 7–8 orders of magnitude compared to 3–4 orders on the packing surface, irreversible bacterial attachment occurred in the liquid itself suppressing the non-specific attachment of bacteria onto the packing surface. When the SB1 exceeded 7 orders of magnitude as reflected by plate counts, the bacteria grew in the liquid rather than on the packing surface, using their inter-attraction to form microorganism floc.

In the third startup, soaking the packing with aeration provided sufficient time for the bacteria to adhere inside of the microporous surface. According to the generation time (0.77–0.87 h) of *Pseudomonas*, prolific SB1 can develop microorganism floc in a sufficient substrate after 24 h. Therefore replacing 50% instead of 30% of the

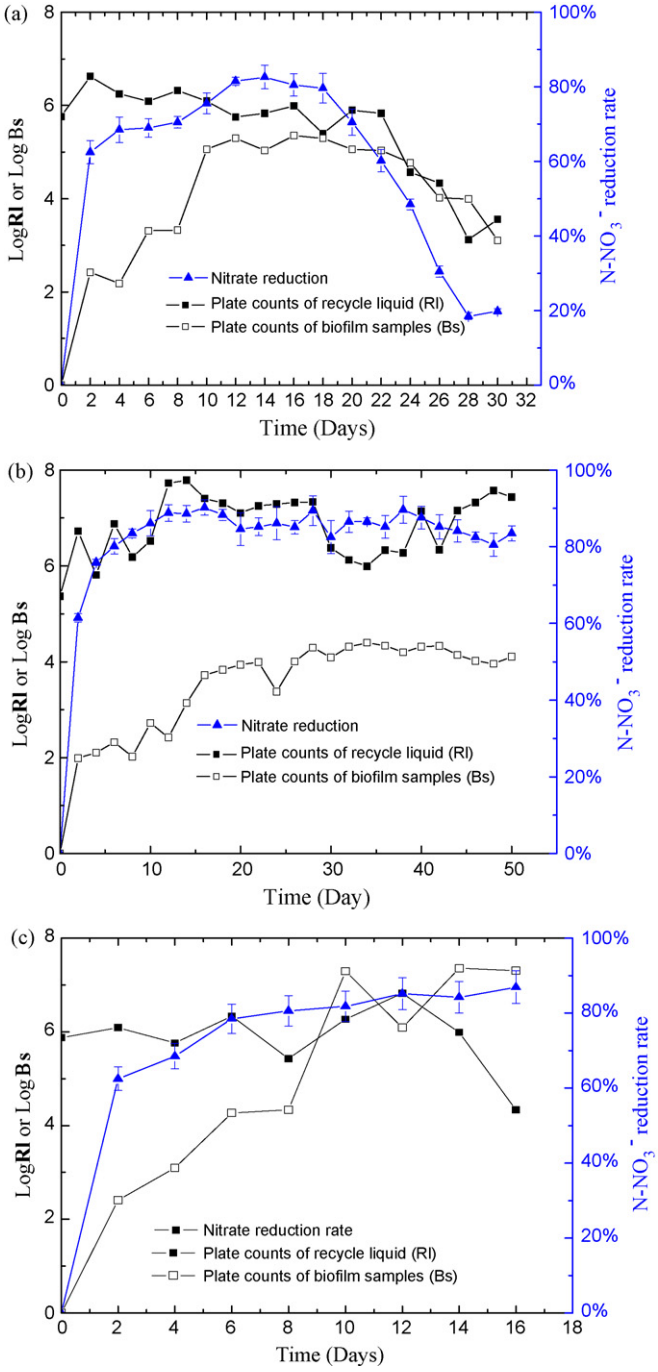

Fig. 4. Plate counts of recycle liquid (RI) and biofilm samples (Bs) with nitrate reduction in three startup strategies, the details of which were shown in Table 2.

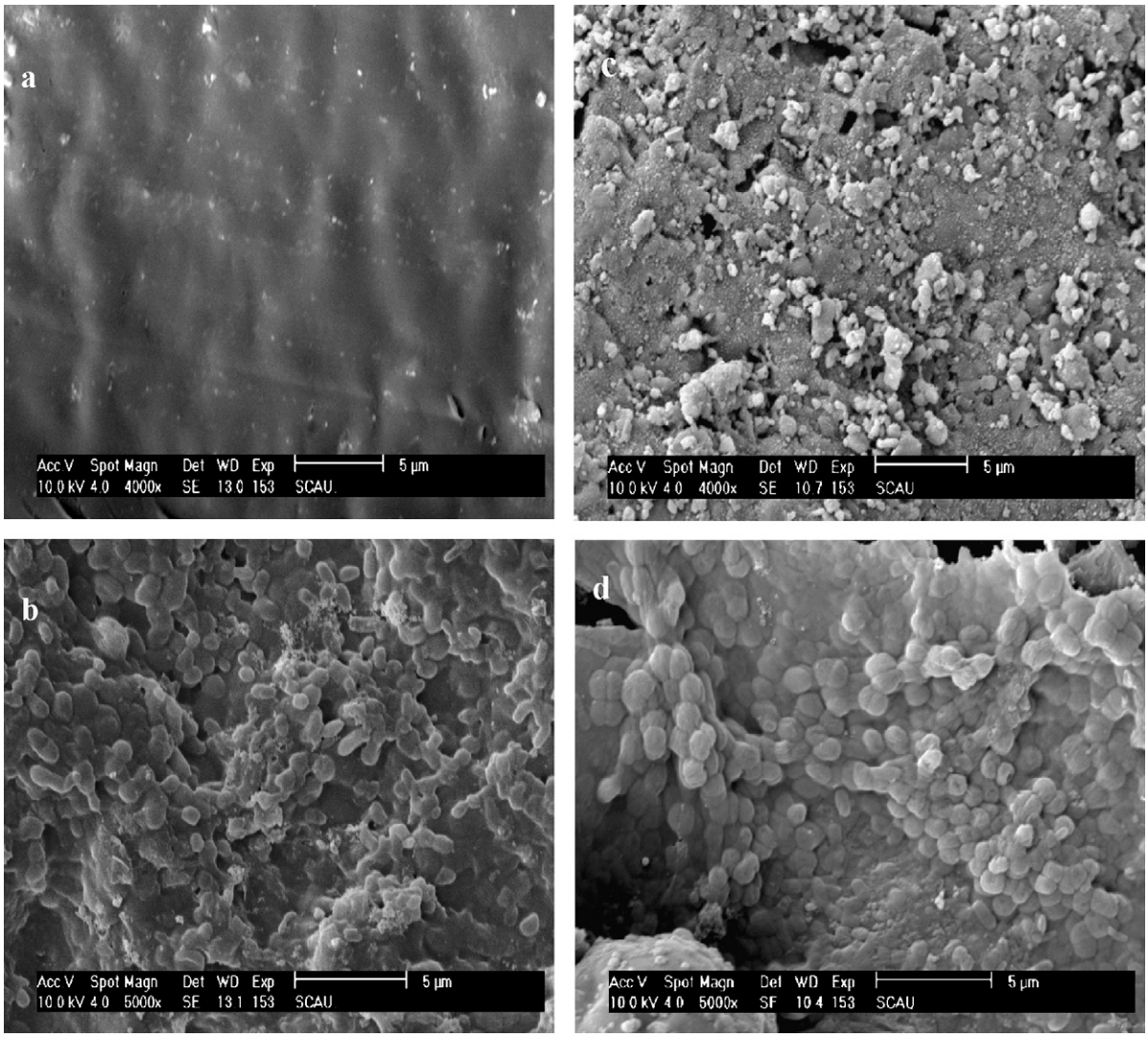

Fig. 5. SEM micrographs of microorganisms grown on the polyhedral spheres surfaces (a) before cultivation, (b) after 40 days of NO treatment, and grown on the ceramic beads surfaces (c) before cultivation and (d) after 40 days of NO treatment.

trickling liquid in the reservoir (C) every other day provided more opportunities for non-specific attachment to the packing surface. A yellow, 50–70 μm thick biofilm formed while the system maintained up to a 90% denitrifying rate at the end of 20 days (Fig. 4c). Although extensive work has been performed on microbial adhesion, many aspects of this process are still unclear, specifically the forces that determine the interactions of microorganisms and support surfaces. Perhaps replacing 60 or 70% trickling liquid might be even more effective. Considering the diversity of the factors influencing the cell adhesion, the spontaneous biofilm formation and the interactions of support – bacteria – liquid, a laborious empirical approach will be necessary to find an optimal startup method for biofilm-based reactors.

3.3. Surface morphology of the packing and biofilm

To confirm the formation of a suitable packing surface biofilm layer, two samples, one of polyhedral spheres and the other of ceramic beads were taken from sample port 2 for analysis after 40 days of NO treatment. The surface characteristics of the samples and of the control were observed by SEM. Fig. 5 shows the microbial communities on the samples before inoculation (a and c) and after 40 days (b and d). It was determined that a mature biofilm had formed after 40 days of operation maintaining a steady 80% NO removal rate in comparison with the control. A comparison of Fig. 5a and c shows that the surface of the polyhedral spheres is smooth while that of the porous ceramic beads is rough. The biofilm formed on the polyhedral spheres (Fig. 5b) is also smooth, giving a flat layer consistent with the flat plate model [27]. In contrast, the rough irregularities in the ceramic beads were magnified. Those protuberances might have reached into regions of higher NO concentration in the three-phase interface microenvironment, growing faster and becoming ever more protuberant.

3.4. Performance during long-term operation

A counter-current BF packed with inert material was started and operated for more than 6 months with a variable NO load and oxygen content (Fig. 6). The injected gas flow rate was 1 L/min, corresponding to an empty bed residence time (EBRT) of 1.5 min in a 1.5 L packed volume. The nitrate concentration was modified during this period in order to promote an alternative metabolism pathway in which NO was used as a nitrogen source under different conditions. KNO_3 (initial 0.5 g/L) was added to the nutrient liquid, while

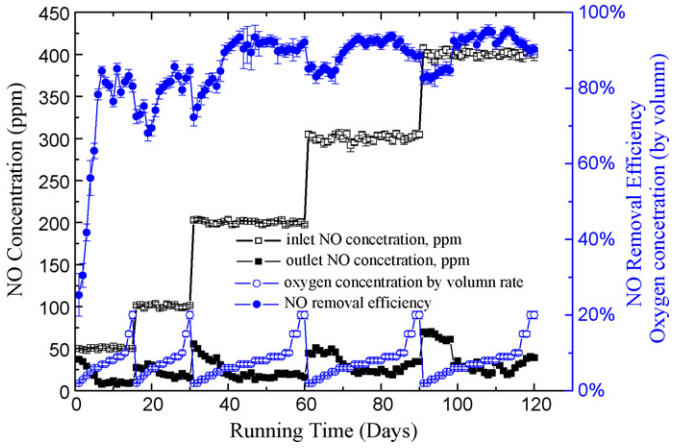

Fig. 6. The performance of the biotrickling filter for NO removal with different oxygen and NO loading (T = 30 °C, inlet gas was 1 L/min, the trickling rate was 150 mL/min, the total trickling nutrient liquid was replaced every other day).

the other ingredients were the same as those used in the startup. During the long-term operation, all the trickling liquid was replaced by fresh nutrient liquid every 2 days to stimulate better cell growth during feeding with NO. The NO removal efficiency in the BF system, consisting of the BF and the humidifier, was defined as

$$\text{RE}\ (\%) = \left(\frac{1 - [\text{NO}]_g^{\text{in}}}{[\text{NO}]_g^{\text{out}}}\right) \times 100 \quad (1)$$

where $[\text{NO}]_g^{\text{in}}$ and $[\text{NO}]_g^{\text{out}}$ are the measured NO concentrations in the inlet and exit gas of the system.

In the first few days of operation, NO RE abruptly decreased to only 25.3% with inlet 50 ppm NO. During the following few days the removal efficiency remained low as a consequence of NO injection. This low level might be caused by the sensitivity of strain SB1 to different nitrogen sources, since the nitrogen source was switched from nitrate to NO. A secondary reason was that the transfer of NO from gas to biofilm was limited by diffusion resistance due to its very low solubility. Once the bacteria adapted themselves to this metabolism pathway, removal efficiency reached a stable rate of approximately 78% after 6 days. From day 6 on, the KNO_3 in the nutrient liquid was reduced to 0.1 g/L. As more O_2 was injected, more NO was oxidized to NO_2. As a result, N-NO_3^- in the trickling liquid increase to above 15 mg/L (10% O_2, 50 ppm NO), after which KNO_3 no longer needed to be added in the nutrient liquid. The NO removal efficiencies were 68.5 ± 20.4, 78.0 ± 5.5, 88.0 ± 5.8 and 89.4 ± 3.4%, with influent feed of 50.3 ± 1.1, 100.8 ± 1.7, 200.5 ± 1.6 and 300.7 ± 4.2 ppm NO, 2–20% oxygen, respectively, showing an increasing NO RE.

Next, the NO load was gradually increased to 32.14 g/m^3 h, corresponding to 400 ppm. At this gas rate 1 L/min, 85–94% RE was reached and maintained for 23 days except for one relatively poorer NO removal (82.5%) caused by abruptly increasing the NO loading. The high performance of the filter was likely due to both the mature biofilm and the high cellular activity that was maintained in an aerobic environment. During this time, the polyhedral spheres became wrapped with a dark, grey biofilm, whose thickness reached 100–150 μm. Although the growing biofilm layer probably lessened the void rate of the filter bed, the pressure drop was steady and small, reaching maximum values of 447 Pa/m. This was partly due to the appropriate void rate of the mixed packing material and the small removal of the biomass when feeding the liquid solution to the reactor. The pH of the BF usually remained between 7.2 and 8.5 as a consequence of denitrification, consistent with the pH development trend of SB1 seen in Fig. 2.

3.5. Effect of oxygen on NO removal

The effect of O_2 concentration from 2 to 20% on NO removal was investigated. The results are presented in Fig. 7. Six to 10% oxygen, which falls within the range actually found in flue gas, was maintained for 4 days to study system stability. All the other O_2 concentrations were sustained for 2 days. The NO RE was not proportional to the inlet O_2 concentrations; as the system maintained a NO RE above 80% in different O_2 concentrations and 400 ppm NO. This was especially significant for O_2 concentrations above 6%, since such a situation would increase the dissolution of oxygen in the moving layer of water in the biofilter, and thus likely promote the strain aerobic nitrogen dissimilatory process. The NO RE ranged from 82.9 to 94.2% and was maintained at 94% for 5 days in 8–9% O_2 concentrations. This corresponds to NO elimination capacities in the BF system ranging from 26.7 to 30.2 g/m^3 h. The NO elimination capacity (EC) was defined as

$$\text{EC} = \text{flow} \times \left(\frac{[\text{NO}]_g^{\text{in}} - [\text{NO}]_g^{\text{out}}}{\text{filter bed volume}}\right) \quad (2)$$

The estimated biological NO removal was calculated as the total RE minus those in the abiotic experiment.

NO is subject to oxidation by O_2. The gas-phase thermal conversion of NO to NO_2 is given by the following equation:

$$2\text{NO}_{(g)} + \text{O}_{2(g)} \rightarrow 2\text{NO}_{2(g)} \quad (3)$$

The rate of oxidation of NO to NO_2 can be expressed by a second-order relationship:

$$\frac{\text{d}[\text{NO}]_g}{\text{d}[t]} = -2k_1[\text{NO}]_g^2[\text{O}_2]_g \quad (4)$$

where the rate constant k_1 is equal to 7.5 × 10^3 L^2/(mol^2 s) at 25 °C [28]. When there is sufficient oxygen, the rate of conversion of NO to NO_2 increases proportional to the square of the concentration of NO.

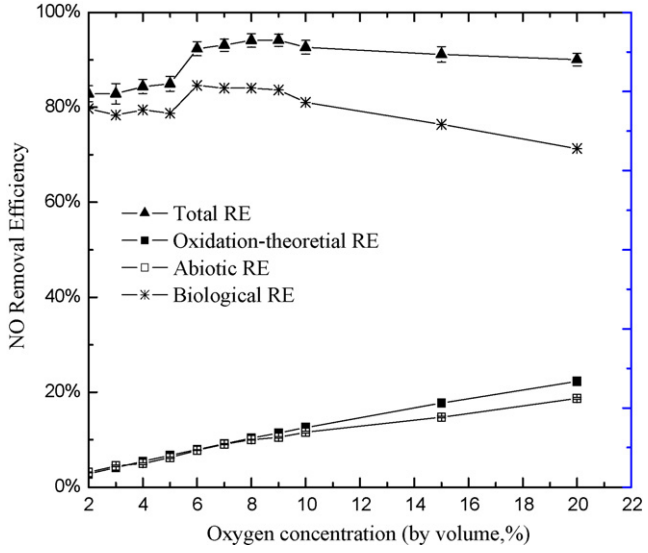

Fig. 7. Abiotic and biological NO removal efficiency (RE) compared with oxidation-theoretical RE estimated by the rate expression in Eq. (7) for a 400 ppm initial NO concentration and varying oxygen concentrations.

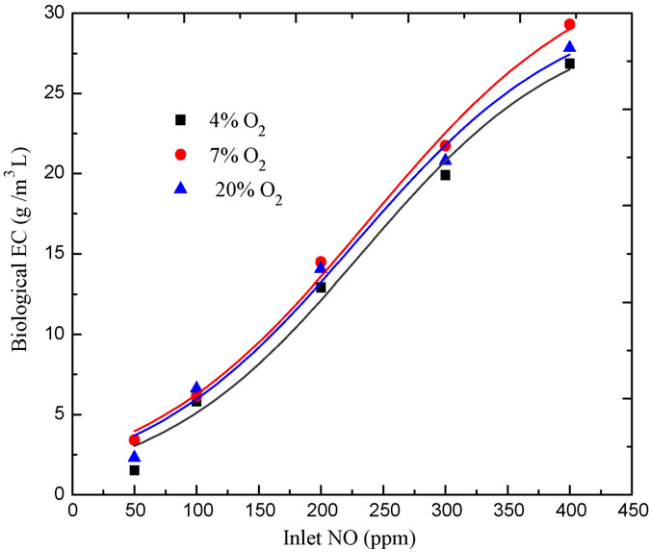

Fig. 8. Biological EC vs. varying inlet NO and O_2. Solid lines show the fit with the logistic cell growth kinetics for 4% O_2 (R^2 = 0.989), 7% O_2 (R^2 = 0.996), and 20% O_2 (R^2 = 0.990).

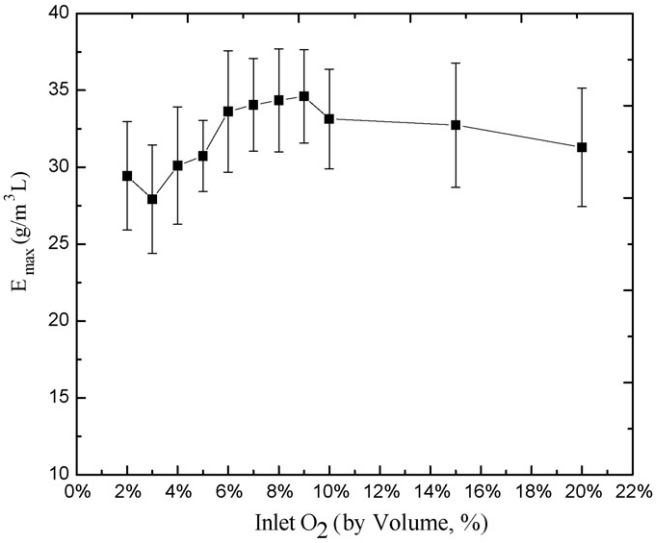

Fig. 9. Effect of O_2 concentration on E_{max} in 50–400 ppm NO (E_{max} is defined in Eq. (12)).

The overall stoichiometric aqueous phase conversion of NO to NO_2 is given by the following equation:

$$4NO_{(l)} + O_{2(l)} + 2H_2O \rightarrow 4NO_{2(l)}^- + 4H^+ \quad (5)$$

$$\frac{d[NO]_l}{d[t]} = -4k_2[NO]_l^2[O_2]_l \quad (6)$$

where the rate constant k_2 is 2.1×10^6 $L^2/(mol^2\ s)$ at 25 °C [28]. A comparison of the reaction rate constants shows that the oxidation of NO in the liquid phase is more rapid than that in the gas phase by almost three orders of magnitude. In this study, the BF was fed gas with almost saturated humidity, and the recycling liquid formed a layer of moving water on the surface of the biofilm, which ensured high water content in the reactor. However, the theoretical aqueous-phase RE is difficult to accurately calculate due to the unknown liquid retention time and wet surface area. Insufficient NO and O_2 transfer from the gas phase to the moving water layer were caused by the low Henry coefficient, which is 21.6 and 34 under the conditions of 20 °C and 1 atm, respectively. The EBRT in the humidifier was 75 s, so a certain portion (about 1.5–15.8%) of NO was naturally oxidized to NO_2 due to the presence of 2–20% oxygen.

According to Eqs. (4) and (6) and the Henry coefficient, the NO RE is mainly dependent on the oxygen concentration as the NO concentration is 400 ppm and there is excessive oxygen in the chemical oxidation. Eq. (7) is based on the assumption that a balance between gaseous NO and aqueous NO was created instantaneously in the BF, and NO_2 would be completely absorb by the trickling liquid:

$$RE_{theory} = \left[\frac{0.01499[O_2]}{1 + 0.01499[O_2]}\right] + \frac{0.003174[O_2]}{(1 + 0.003174[O_2])]} \times 100\%$$

$$0 < [O_2] \leq 20\% \quad (7)$$

The efficiencies above indicate that the existence of significant abiotic oxidation caused a slight increase in RE.

In order to clarify the biological NO removal efficiency, an abiotic experimental removal of NO was carried out in a control reactor with all the other conditions kept the same but without any microorganism to parallel the BF. The abiotic NO removal efficiencies were slightly lower than the calculated removal efficiencies, because of unknown factors such as inadequate oxidation and gas retention in irregular surfaces which would affect the gas phase reactor in non-plug flow condition. Another cause might be a slight addition of NO in the residence time caused by a side-reaction:

$$2NO_{2(g)} + H_2O \rightarrow HNO_3 + HNO_2, \qquad \Delta G^\circ = -1.85\ kJ \quad (8)$$

$$3NO_{2(g)} + H_2O \rightarrow 2HNO_3 + NO_{(g)}, \qquad \Delta G^\circ = -3.01\ kJ \quad (9)$$

From reactions (8) and (9), it can be noted that reaction (8) involves a higher standard Gibbs's free energy than reaction (9). As a result of the more favorable reaction (9), NO is released into the system. This may also be the reason why NO RE rarely reaches more than 95%.

Approximately 79.3% of the total removal was due to microbial aerobic denitrification, while abiotic oxidation to NO was most efficient when the inlet flue gas injected 20% oxygen. Yang's study [29] showed that NO removal was remarkable under anaerobic conditions and could reach 99%. In contrast, under aerobic conditions, only about 60% removal was achieved. In this study, the estimated biological NO removal ranged from 71.4 to 84.6%, and exceeded 84% when the oxygen concentration was 6–8% (Fig. 7). Thus, the oxygen had no negative effect on the aerobic denitrifier SB1, but rather enhanced the total efficiency in part due to chemical oxidation and in part due to the strain activities.

3.6. A kinetic study of the oxygen concentration and biological NO removal

A kinetic study of the oxygen concentration and biological NO removal is described by the logistic equation based on NO as the growth substrate. The logistic equation [30] describing cell growth, production formation, and substrate consumption is as follows:

$$\frac{dX}{dt} = \mu_{max} X \left(\frac{1 - X}{X_{max}}\right) \quad (10)$$

where μ_{max} is the maximum specific growth rate of the microorganisms; X is the concentration of cells; X_{max} is the maximum value of the cell concentration; and t is the cultivation time. After integration, Eq. (10) becomes

$$X = \frac{X_{max}}{(X_{max} - X_0)e^{-\mu_{max} t} + 1} \quad (11)$$

In this macroscopic system, the initial NO removal efficiency decreased (Fig. 6) during every step of the NO increase. The phenomena indicated an initial insufficient biomass in the BF, even though the increase in the inlet NO concentrations would enhance the driving force for mass transfer. Moreover, it was observed that the BF system took a few days to reach a new steady state. For low concentrations of contaminant, the biomass growth is directly proportional to the contaminant concentration [27]. The proposed NO removal model of Eq. (12) is based on the following assumptions:

(1) The logistic equation describes strain SB1 growth in the BF.
(2) The inlet NOx has only NO with no NO_2.
(3) The NOx biological removal reaction only occurred in the biofilm.
(4) The NO removal efficiency was proportional to the biomass concentration in the BF, such that: $dX/dt \propto dE/dt$.
(5) The only substances affecting the rate of biodegradation is NOx, assuming other nutrients are abundant. $dX/ds \propto dE/ds$, where dX/ds is the microorganism growth rate due to consumption of the growth substrate.

Thus

$$E = \frac{E_{max}}{(E_{max} - E_0)e^{-\beta_{max}C} + 1} \quad (12)$$

where E is biological EC, E_{max} is the maximum value of biological EC in a specific condition, C is the NO concentration, and β_{max} is the maximum specific EC increasing rate. The E_{max} and β_{max} were determined by fitting Eq. (12) to the experimental data using Origin (Version 7.5). The nonlinear least squares fitter tool was used to find the equation parameters. The relationship in E and C for different oxygen concentrations fit Eq. (12) well, while the coefficient of determination (R^2) is above 0.9 (Fig. 8). The values of E_{max} exceeded 34 g/m^3 h in the range of 7–9% oxygen, which is within the actual range of oxygen concentrations in flue gas. In this inlet oxygen range, both the simulation data (Fig. 9) and biological RE (Fig. 7) were high as result of the special high denitrifying activities in the DO environment. It confirmed that NO removal caused by microbial metabolism could be predicted by our equation under different inlet concentrations.

4. Conclusions

The general results of the present study demonstrate that denitrification removal of NO by a BF inoculated *P. putida* SB1 is an effective protocol for eliminating NOx from flue gas. The newly isolated strain SB1 has a high denitrifying ability, removing 95% of the nitrate in a 24 h period in an aerobic environment, with no accumulation of nitrite. In addition, soaking the packing with aeration provided sufficient time for the bacteria to adhere to the microporous surface in startup. Replacing 50% of the trickling liquid was an effective strategy of starting the biosystem.

The BF system was able to remove 82.9–94.2% NO consistently when the inlet NO was 400 ppm in an enriched oxygen stream of 2–20%. A kinetic relation between the oxygen concentration and biological NO removal was developed to confirm that the microbial metabolism played the main role in denitrifying removal NO. Moreover, both the simulated maximum biological EC and experimental biological RE were high as the inlet oxygen was within the possible range of oxygen concentrations in flue gas.

Overall, the results presented and discussed herein clearly indicate the feasibility of the BF for denitrifying removal of NO in flue gases conditions.

Acknowledgements

This research was financially supported by National Natural Science Foundations of China on air quality improvement (Grants No. 20777019) and the Science & Technology Project of Guangdong Province.

Appendix A. Supplementary data

Supplementary data associated with this article can be found, in the online version, at doi:10.1016/j.jhazmat.2008.08.058.

References

[1] S. Barman, L. Philip, Integrated system for the treatment of oxides of nitrogen from flue gases, Environ. Sci. Technol. 40 (2006) 1035–1041.
[2] F.H. Zhu, Electric power industry development and environmental protect, Electric Power Environ. Protect. 22 (2006) 1–7.
[3] Y. Jin, V.M. Veiga, C. Kennes, Bioprocesses for the removal of nitrogen oxides from polluted air, J. Chem. Technol. Biotechnol. 80 (2005) 483–494.
[4] P. Van Der Maas, P. Van Den Bosch, B. Klapwijk, P. Lens, NOx removal from flue gas by an integrated physicochemical absorption and biological denitrification process, Biotechnol. Bioeng. 90 (2005) 234–244.
[5] D.S. Jin, B.R. Deshwal, Y.S. Park, H.K. Lee, Simultaneous removal of SO_2 and NO by wet scrubbing using aqueous chlorine dioxide solution, J. Hazard. Mater. 135 (2006) 412–417.
[6] W. Li, C.Z. Wu, S.H. Zhang, Evaluation of microbial reduction of Fe(III)EDTA in a chemical absorption-biological reduction integrated NOx removal system, Environ. Sci. Technol. 41 (2007) 639–643.
[7] H.H.J. Cox, Z.M. Shareefdeed, M.A. Deshusses, Thermophilic biotrickling filtration of ethanol vapors, Environ. Sci. Technol. 35 (2001) 2612–2619.
[8] L. Philip, M.A. Deshusses, Sulfur dioxide treatment from flue gases using a biotrickling filter-bioreactor system, Environ. Sci. Technol. 37 (2003) 1978–1982.
[9] L. Philip, M.A. Deshusses, The control of mercury vapor using biotrickling filters, Chemosphere 70 (2008) 411–417.
[10] J.M. Barnes, W.A. Apel, K.B. Barrett, Removal of nitrogen oxides from gas stream using biofiltration, J. Hazard. Mater. 41 (1995) 315–326.
[11] E. Chagnot, S. Taha, G. Martin, Treatment of nitrogen oxides on a percolating biofilter after pre-concentration on activated carbon, Process Biochem. 33 (1998) 617–624.
[12] W.P. Flanagan, W.A. Apel, W.A. Barnes, J.M. Lee, Development of gas phase bioreactors for the removal of nitrogen oxides from synthetic flue gas streams, Fuel 81 (2002) 1953–1961.
[13] B.D. Lee, W.A. Apel, W.A. Smith, Oxygen effects on thermophilic microbial populations in biofilters treating nitric oxide containing off gas streams, Environ. Prog. 20 (2001) 157–167.
[14] D. Patureau, E. Zumstein, J.P. Delgenes, R. Moletta, Aerobic denitrifiers isolated from diverse natural and managed ecosystems, Microb. Ecol. 39 (2000) 145–152.
[15] J.J. Su, B.Y. Liu, C.Y. Liu, Comparison of aerobic denitrification under high oxygen atmosphere by *Thiosphaera pantotropha* ATCC 35512 and *Pseudomonas stutzeri* SU2 newly isolated from the activated sludge of a piggery wasterwater treatment system, J. Appl. Microbiol. 90 (2001) 457–462.
[16] R.W. Ye, A. Arunakumari, Mutants of *Pseudomonas fluorescens* deficient in dissimilatory nitrite reduction are also altered in nitric oxide reduction, J. Bacteriol. 174 (1992) 2560–2564.
[17] D. Patureau, N. Bernet, R. Moletta, Combined nitrification and denitrification in a single aerated reactor using the aerobic denitrifier *Comamonas* sp. Strain SQLY2, Water Res. 31 (1997) 1363–1370.
[18] D. Zart, E. Bock, High rate of aerobic nitrification and denitrification by *Nitrosomonas eutropha* grown in a fermentor with complete biomass retention in the presence of gaseous NO_2 or NO, Arch. Microbiol. 169 (1998) 282–286.
[19] K.C. Loh, T.S. Chung, W.F. Ang, Immobilized-cell membrane bioreactor for high-strength phenol wastewater, J. Environ. Eng. ASCE 126 (2000) 75–79.
[20] E.M. Nkhalambayausi-Chirwa, Y.T. Wang, Modeling Cr(VI) reduction and phenol degradation in a coculture biofilm reactor, J. Environ. Eng. ASCE 131 (2005) 1495–1507.
[21] Y.M. Chen, T.F. Lin, C. Huang, F.M. Hsieh, Degradation of phenol and TCE using suspended and chitosan-bead immobilized *Pseudomonas putida*, J. Hazard. Mater. 148 (2007) 660–670.
[22] N. Takaya, M.A. Catalan-Sakairi, Aerobic denitrifying bacteria that produce low levels of nitrous oxide, Appl. Environ. Microbiol. 69 (2003) 3152–3157.
[23] S. Ozeki, N. Takaya, H. Shoun, A novel Cl-utilizing aerobic denitrifier *Alcaligenes* sp. STC1 and its genes for copper-containing nitrite reductase and azurin, Biosci. Biotechnol. Biochem. 65 (2001) 1206–1210.
[24] W.G. Weisburg, S.M. Bains, D.A. Pelletier, 16Sribosomal DNA amplification for phylogenetic study, J. Bacteriol. 173 (1991) 697–703.
[25] APHA (American Public Health Association), Standard Methods for the Examination of Water and Wastewater, 20th ed., APHA, Washington, DC, 1998.

[26] G. Cheng, Z. Zhang, D. Bryers, Inhibition of bacterial adhesion and biofilm formation on zwitterionic surfaces, Biomaterials 28 (2007) 4192–4199.
[27] J.S. Devinny, J. Ramesh, A phenomenological review of biofilter models, J. Chem. Eng. 113 (2005) 187–196.
[28] H.H. Awad, D.M. Stanbury, Autoxidation of NO in aqueous solution, J. Chem. Kinet. 25 (1993) 375–381.
[29] W.F. Yang, H.J. Hsing, Y.C. Yang, J.Y. Shyng, The effects of selected parameters on the nitric oxide removal by biofilter, J. Hazard. Mater. 148 (2007) 653–659.
[30] H.W. Blanch, D.S. Clark, Biochemical Engineering, Marcel Dekker, Inc., New York, 1997.